



Rapid and sustainable battery health diagnosis for recycling pretreatment using fast pulse test and random forest machine learning



Shengyu Tao^a, Ruifei Ma^a, Yuou Chen^a, Zheng Liang^a, Haocheng Ji^a, Zhiyuan Han^a, Guodan Wei^a, Xuan Zhang^{a, **}, Guangmin Zhou^{a,*}

^a Tsinghua-Berkeley Shenzhen Institute, Tsinghua Shenzhen International Graduate School, Tsinghua University, China

HIGHLIGHTS

- SOH diagnosis for recycling highlights no historical data and high heterogeneity.
- Pulse tests can reveal the SOH while saving time, cost, and carbon emissions.
- 442 retired batteries from lab tests and actual electric vehicle usages are tested.
- The random forest achieves high diagnosis even if limited data is available.
- Combined with the pulse test, the random forest can generalize to unseen data.

ARTICLE INFO

Keywords:

Battery health diagnosis
Battery recycling
Pulse test
Machine learning
Field data
Economic-environmental analysis

ABSTRACT

This research introduces a novel state of health (SOH) diagnosis method for retired lithium-ion batteries (LIBs) in recycling pretreatment, employing a fast pulse test and random forest machine learning. We highlight the SOH diagnosis for recycling as a highly heterogeneous and no-historical-data issue. A diverse out-of-distribution dataset is collected from 442 retired commercial LIBs, originating from 4 manufacturers, 2 physical formats, 5 capacity designs, and 9 historical usages. Following the pulse test, key features are identified from the voltage response and utilized to instruct machine-learning models. The SOH diagnosis error rates are 1.30% and 1.79%, without any prior knowledge of the historical usage pattern, for training and testing, respectively. Moreover, models can generalize to different capacity designs, cathode materials, and even unseen datasets. Pulse tests substantially curtail the requisite testing time by a minimum of 70%, in comparison to the regular 1A capacity calibration, resulting in a noteworthy economic and environmental advantage. Assuming the SOH of the retired batteries to be 0.5, pulse tests save up to 1443.7 yuan (201.02 dollars) and reduce 65.43kg of CO₂ emissions per ton of retired batteries. The findings bolster the efficiency of battery recycling pretreatment, promoting the overall profitability and sustainability of recycling.

1. Introduction

Lithium-ion batteries (LIBs) have emerged as a critical technological cornerstone, playing a pivotal role in various sectors due to their superior energy density and long cycle life [1]. Nevertheless, LIBs are deemed unfit for critical applications, such as electric vehicle (EV) usage, when their state of health (SOH) falls below a certain threshold, i.e., 80% of the nominal capacity. This is due to the capacity fade and increasing internal resistance over the lifetime [2], resulting in reduced

driving range, increased charging time, and potential safety hazards, not allowed for daily EV operation. Discarding the end-of-life EV batteries, however, poses a considerable waste of resources and intensive carbon footprint due to premature retirement [3].

Given that retired batteries may retain up to 80% of the initial capacity, they can be deemed useful for other less demanding applications, contrary to their premature retirement. Ladder utilization and battery recycling present potential solutions for addressing the premature retirement of LIBs. Ladder utilization involves re-purposing these retired

* Corresponding author.

** Corresponding author.

E-mail addresses: xuanzhang@sz.tsinghua.edu.cn (X. Zhang), guangminzhou@sz.tsinghua.edu.cn (G. Zhou).

batteries in stationary energy storage applications [4], whereas battery recycling entails the extraction and recovery of valuable materials from retired batteries [5–7]. While ladder utilization is currently suitable for pilot programs due to safety concerns, battery recycling is scaling up thanks to economic viability [8]. Battery recycling, however, is highly SOH-sensitive, with the efficiency and profitability of the recycling process hinging on the accurate diagnosis of battery SOH information [9]. Misjudgment of SOH could lead to sub-optimal recycling route design, resulting in wasted chemical reagents and deteriorated product quality [10]. Therefore, access to SOH information is indispensable for profitable and sustainable battery recycling [11].

The traditional SOH diagnosis for EV usage has been well-studied, including columb counting [12], electrochemical model [13], empirical model [14], impedance spectroscopy [15], data-driven model [16], and their combinations. These methods share the common core idea that one could leverage hidden patterns in historical data to fit the future battery SOH either in a mechanism-driven or data-driven way. However, SOH diagnosis at the battery recycler's end is a backward-looking problem, where the historical data is typically unavailable [17]. An intuitive way is to perform a calibration test to get capacity retention. Jiang et al. applied 0.1C (6A) constant current to obtain the voltage curve of the LIBs repurposed in power grid frequency regulation and peak shaving applications, using incremental capacity (IC) features to obtain SOH and resulting in a capacity calibration time over 20h [18]. In contrast to a regular full charging/discharging test, cell/pack cycling data (i.e., specific capacity and voltage profile) can serve as a diagnosis of active lithium loss and basic battery integrity assessment [19]. Xin et al. used voltage response in the partial charging stage to sort the retired LIBs, which equivalently saved over half of the testing time [20]. Braco et al. further simplified the partial charging method by extracting health indicators within a voltage range from 3.7V to 4.15V with a resolution of 5mV, to find relevant patterns in the early voltage response stages [21] and reported the robustness of voltage response under different scenarios [22]. Considering internal resistance has rich degradation information, Mona et al. combined electrochemical impedance spectroscopy and Gaussian process regression to estimate the SOH of the second-life LIBs [23]. Even though the test can be finished within a few hours, it is still costly and time-consuming to capture the low-frequency region pattern due to the large time constant of the mass transport process [24]. It is noted that electrochemical impedance spectroscopy can be interpreted differently when the state of charge (SOC) varies. Fan et al. performed an electrochemical impedance spectroscopy test at 5% SOC on the retired power batteries, thus saving long data acquisition time that was otherwise needed for higher SOC levels [25]. Another significant difference between SOH diagnosis for first-life and recycling scenarios is that the latter typically encounters considerable heterogeneity in terms of cathode chemistries, historical usages, cell-to-cell inconsistency, physical formats, capacity designs, and SOH distributions, which challenges diagnosis tasks [22,26–30,39]. Therefore, Ran et al. first clustered similar retired batteries and then estimated remaining capacities for clustered batteries with a two-step learning method combining a pulse test [31] and reported a robust result when using an inter-cycle shift in voltage response as a health indicator in a wide SOC range [32]. However, such a shift still requires substantial testing time to retrieve. Consequently, the testing time issue rigidifies the difficulty where SOH information is critical to determine the reagent dosage but is expensive to test. Such a difficulty calls for studying the SOH diagnosis, especially for battery recycling pretreatment, in a rapid, accurate, and highly heterogeneous fashion.

In this research, we investigate the SOH diagnosis for recycling pretreatment, highlighting only using the field available data rather than the historical operational data. To this end, we collect 241 retired commercial LIBs from 2 manufacturers, 2 physical formats, 3 capacity designs, and 7 historical usages to build a diversified out-of-distribution dataset. In contrast to performing a regular charging/discharging test, we apply a fast pulse test to map the battery aging status. Simple yet

effective features from the voltage response curve are extracted. To tackle heterogeneities, we deliberately mix up the features extracted from different retired batteries to train generalized machine learning models. Furthermore, we perform an economic-technical analysis of the carbon benefit and cost (profit) using a pulse test for SOH pretreatment in hydrometallurgical, direct, and pyrometallurgical recycling settings, respectively. Our core idea is summarized in Fig. 1, which highlights the advantages of fast testing time, low electricity consumption, and high carbon benefits. Such advantages need no prior information on historical usage and are robust for diversified retired batteries.

The rest of this article is organized as follows. The second section introduces the experimental method including the data acquisition and machine learning method. The third section presents the results and discussion on data visualization, prediction performance, and economic-environmental analysis. The last section concludes and discusses this research.

2. Method

In this section, we introduce the data acquisition, dataset generation, and the machine learning method.

2.1. Data acquisition

We have collected two parts of data, including the lab-testing cells with accelerated aging experiments and actual cells retired from electric vehicles. The overall data size is 442 samples. For the first part, we have collected 218 cylindric and 23 pouch retired $\text{LiNi}_{1-x-y}\text{Co}_x\text{Mn}_y\text{O}_2$ samples. For cylindric retired batteries, nominal capacities are 2.6Ah and they follow the same manufacturing standard. The batteries are yet manufactured in six different batches, and we, therefore, name the batteries as CylinB1, CylinB2, CylinB3, CylinB4, CylinB5, and CylinB6, respectively. For the second part, the cathode material types are LMO and NCM, with a nominal capacity of 10Ah and 21Ah, respectively. Such a capacity design is notably larger than those of lab-testing cells, bringing more diversities in capacity designs. We purchased retired batteries from battery recyclers for further testing. These batteries are retired from EV applications and have different historical usages, but we do not require knowledge of the explicit state, which increases the diversity of battery health states. In Table 1, the information on the parameter setting of the pulse test for actual cells retired from electric vehicles is listed. It is noted that the NCM group has some batteries with a capacity larger than the nominal capacity, which could be attributed to the capacity recovery phenomenon of some less degraded batteries after a long period of rest. We also test these retired batteries under two pulse width settings, i.e., 5s and 10s, which will be elaborated on in the following sections.

The definition of SOH under the battery recycling setting is different from that of the EVs. Specifically, the EV setting highlights the access to the historical operation conditions when calculating SOH thus a whole SOH trajectory can be obtained. On the contrary, the battery recycling setting has no access to the historical operation data thus only a scalar SOH at the end-of-life point is calculated for each retired battery. Herein, we define the SOH of a retired battery as:

$$\text{SOH} = \frac{C_{EOL}}{C_{nom}} \quad (1)$$

where, the C_{EOL} is the capacity of a retired battery at the end-of-life point, equivalently, the capacity when the retired battery is collected by the battery recycler. Note that the C_{EOL} is a scalar value rather than a consecutive SOH trajectory as in EV applications. The C_{nom} is the nominal capacity of the retired battery.

Given that lab-testing batteries are retired from different historical usages, SOH distributions spread in a wide range, specifically, from 0.4 to 0.95. For pouch batteries, nominal capacities are 5.2Ah and 3.1Ah,

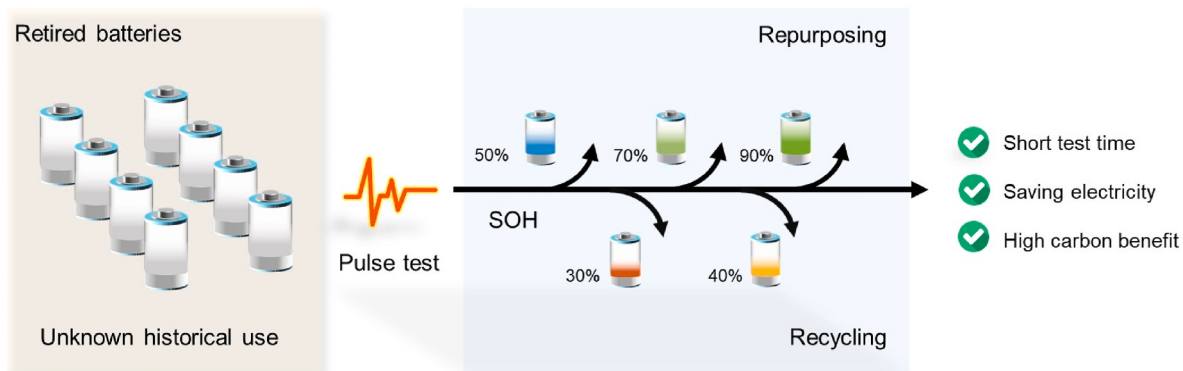


Fig. 1. The concept of rapid SOH diagnosis for retired batteries with unknown and heterogeneous historical use by pulse test and machine learning.

Table 1

The information on the parameter setting of the pulse test for actual cells retired from electric vehicles. The physical format is the pouch.

Cathode	Capacity	Pulse width	Battery health	Pieces
LMO	10Ah	5s/10s	0.65–0.92	50/50
NMC	21Ah	5s/10s	0.90–1.01	50/51

respectively. It is noted that the 23 pouch retired battery samples are deliberately generated from two 3.1Ah and three 5.2Ah batteries. Specifically, we take the capacity values from one single battery, yet in different cycles as unique battery samples such that we can control the SOH distribution in a similar range, from 0.5 to 0.95. Since we do consider historical usages, the cycling scheme for the pouch batteries is not elaborated, but it can be found in Ref. [32]. The generated pouch samples are named PouchB1.

Fig. 2 shows physical illustrations of the battery test platform with different battery testing formats for the lab-testing cells. In Fig. 2(a)–a

sixty-four-channel high-throughput automatic sorting machine invented by Ran et al. [31] is used for pulse test of the retired cylindric batteries. The host PC is responsible for the pulse parameter setting and the data recording. Even if the automatic sorting machine was originally invented to cluster the batteries into similar groups for a convenient capacity diagnosis, here we only use the machine to generate pulses and to build a machine learning model that can be generalized to different battery clusters. In Fig. 2(b), cylindric batteries with different historical usages are fed to the pulse test. Considering the automatic sorting machine is not compatible with pouch formats, we also tested retired pouch batteries using LANHE CT2001A. In Fig. 2(c), the testing station generates the pulse signal and records the battery data. In Fig. 2(d), we position batteries in a climate chamber for safety purposes, but not to control the testing temperature since the temperature response can be neglected in short pulse time.

Fig. 3 demonstrates the data generation and the according feature engineering process. When dealing with retired batteries, initial SOC information is unknown to battery recyclers. In Fig. 3(a), we first

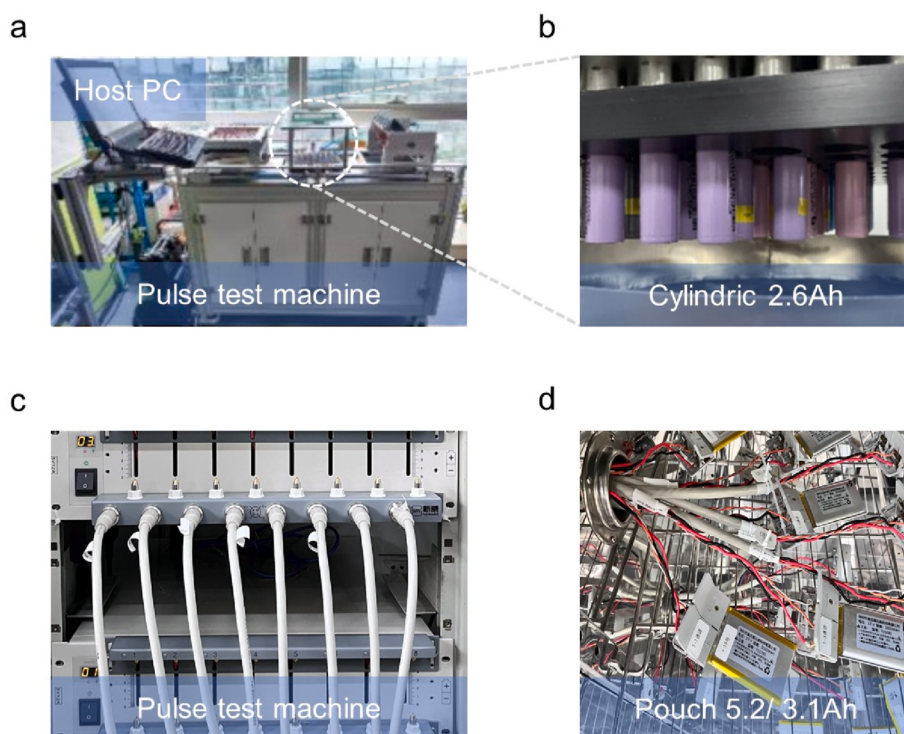


Fig. 2. Physical illustration of the battery test platform. (a) The structure of the pulse test machine for cylindric battery testing. (b) The zoomed-in view of the retired cylindric 2.6Ah batteries fed to test. (c) The pulse test machine for pouch battery testing. (d) The zoomed-in view of the retired pouch batteries under test.

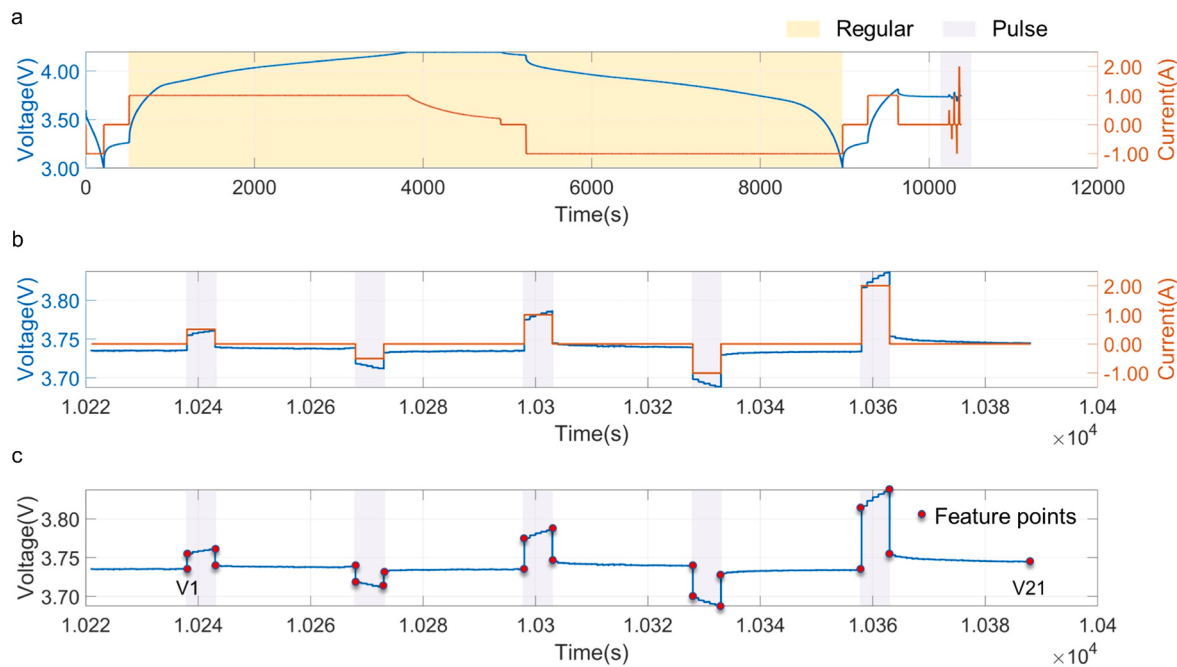


Fig. 3. Dataset generation. (a) Comparison between the regular 1C CC-CV charging/discharging profile and the pulse test. (b) The zoomed-in view of the pulse test. (c) Feature extraction on the voltage response in pulse test. All the tests are performed under room temperature, i.e., 25°C.

discharge retired batteries to the 3V using a 1C constant current. Then a 1C CC-CV charging and a 1C CC discharging are performed for benchmarking the real capacity of the retired batteries. Specifically, a constant voltage at 4.2V with a C/200 cutting-off current is set, followed by a 300s rest. The cutting-off voltage for discharging is 3V, followed by a 300s rest. After the regular capacity benchmarking, we perform the pulse test. Given SOC range poses a significant influence on the voltage response, we select 5% SOC with two considerations: (1) such a SOC level has been reported to be effective in depicting battery degradation status [25], and (2) a low SOC range will save extra charging time before the pulse test is performed. It is noted that the SOC information of retired batteries is not known as a priori under battery recycling scenarios, we alternatively charge the retired batteries for 180s to obtain the SOC level around 5% using a 1C constant current, followed by a 600s rest. Even though such a 1C constant current does not necessarily lead to an accurate 5% SOC of the current battery capacity, we highlight the effectiveness of the pulse test under low SOC regions and the time saved by charging to higher SOC regions. In Fig. 3(b), a zoomed-in view of the pulse test and voltage response is illustrated. The pulse scheme is as follows: (1) Pulse 1 (P1), charge with 0.5C for 5s, and rest for 25s; (2) Pulse 2 (P2), discharge with 0.5C for 5s, and rest for 25s; (3) Pulse 3 (P3), charge with 1C for 5s, and rest for 25s; (4) Pulse 4 (P4), discharge with 1C for 5s, and rest for 25s; (5) Pulse 5 (P5), charge with 2C for 5s, and rest for 25s. We have additionally tested the actual retired cells from electric vehicles with pulse widths of 10s under the same current amplitude setting.

Considering that voltage responses effectively capture the battery degradation information [33], we extract features from the voltage response signals when pulses are applied. Ran et al. processed such raw voltage response data by applying a principal component analysis transformation aiming at dimension reduction. They successfully reduced the dimension of the otherwise over 6000-dimensional raw data to one feature that captured over 95% of the information variance and another two calculated features. However, such a transformation only captures the latent pattern hidden in the original data and poses challenges in model interpretation. Herein, we manually extract features from the voltage responses of each pulse applied as opposed to performing any latent transformation while reducing data dimension. In

Fig. 3(c), turning points of voltage response are regarded as features. As a result, 21 feature points, i.e., V_1 to V_{21} , are extracted from five applied pulses for machine learning models.

2.2. Machine learning framework

The SOH diagnosis is a regression problem, characterized by a substantial degree of complexity and heterogeneity at the recycling end. The features manifest a high divergence due to an array of reasons, including manufacturing variations, disparate historical usages, and inconsistent formats. Such variability leads to a high degree of data heterogeneity, making traditional linear regression techniques inadequate for the task. To address this, we use the random forest, which has proved advantageous in handling heterogeneous and high-dimensional data due to its ensemble learning nature [34]. Define the feature matrix and the label vector as $X \triangleq [V_1^m, \dots, V_n^m]_{m \times n}$ and $y_{m \times 1}$, where m and n are the sample size and feature dimension, respectively. For instance, each row in X and y stands for a unique feature vector and scalar SOH label of the retired batteries, respectively. We randomly split the training/testing set as 8:2 and also ensured that all the battery types were presented in training/testing sets, respectively. The random forest for regression can be formulated as:

$$\bar{y} = \bar{h}(X) = \frac{1}{K} \sum_{k=1}^K h(X; \theta_k, \theta_k) \quad (2)$$

where \bar{y} is the predicted SOH value vector. Note that the predicted SOH \bar{y} is also an m by 1 column vector, which is constituted by the predicted SOH values of m retired battery samples rather than m consecutive SOH values of one battery in different aging status. K is the tree number in the random forest. θ_k and θ_k are the hyperparameters, i.e., the minimum leaf size and the maximum split of the k th tree in the random forest, respectively.

To find the correlation between the j th extracted features and the SOH vector y , the Pearson correlation $\rho_{X_j, y}$ is calculated as:

$$\rho_{X_j, y} = \frac{\text{cov}(X_j, y)}{\sigma_{X_j} \sigma_y} \quad (3)$$

where cov and σ are the covariance operator and the standard deviation operator, respectively. X_j is the j th feature, i.e., V_j^m .

We use an error rate Err (%) to evaluate the model performance:

$$\text{Err} (\%) = \frac{1}{m} \sum_{i=1}^m \frac{|y_i - \bar{y}_i|}{y_i} \times 100 \quad (4)$$

where m is the sample size and y_i and \bar{y}_i are the i th true and predicted SOH values. Bayesian optimization is used to minimize Err (%) by searching optimal hyperparameters of the random forest. The search range is integers from 1 to 100 for all hyperparameters. The maximum iteration is set as 30. We use the optimized model for the result analysis and interpretation.

3. Results and discussion

In this section, we present the statistical analysis of the extracted features, the prediction performance of the machine learning model, and the economic-environmental analysis of the pulse test.

3.1. Statistical analysis

The difficulty of SOH diagnosis under battery recycling scenarios is attributed to the heterogeneous data distribution in cathode material types, manufacturing variabilities, historical usage patterns, physical formats, and subsequent SOH distributions. In Fig. 4(a), we visualize the SOH points in each group of retired batteries. Most SOH points are concentrated in specific SOH regions, which adheres to the fact that all the batteries in each group are subject to the same application purpose. Despite concentrated SOH values in each group, we deliberately mix the battery data across all groups to train a generalized model as opposed to training models for each group. Since battery design parameters and historical usage conditions of each group are the same, the battery

capacity is expected to be concentrated in a small range. Therefore, outliers in each group can be considered as a degradation mechanism shift, which is usually an inconsistency caused by variability in the manufacturing process or grouping strategies. Even though it is a very challenging task to require a battery with known and varying degradation mechanisms, our work still hopes to add the possibility of including more degradation mechanisms to the training data without explicitly knowing the historical usage status of retired batteries. Specifically, CylinB1, CylinB3, CylinB4, and CylinB6 groups have several outliers, where major aging mechanism shifts could take place, however, we keep these samples since we want to train a generalized model even if the retired batteries are subject to different aging mechanisms. The median SOH values from CylinB1 to CylinB6 groups are 0.84, 0.94, 0.75, 0.61, 0.78, and 0.5, respectively. As introduced in Section 2.1, the SOH samples of pouch batteries are taken from several unique batteries at their different cycles. Therefore, a wide SOH distribution from 0.5 to 0.95 can be observed.

In Fig. 4(b), we analyze the Pearson correlation between the group-wise SOH and the group-wise feature value. For instance, the group-wise feature values of V_1 , V_2 , V_3 , and V_4 are obtained from the first pulse, showcasing a consistent negative correlation with the group-wise SOH. Specifically, the Pearson correlation is -0.89 , -0.85 , -0.85 , and -0.89 for the features V_1 , V_2 , V_3 , and V_4 , respectively. It means that retired batteries tend to exhibit a higher voltage response value when in lower SOH status, which adheres to the physical knowledge of the degradation of LIBs. LIBs undergo physical and chemical transformations with aging, leading to capacity loss and subsequent SOH decrease. A key aging effect is formation of solid electrolyte interphase on electrode surfaces, contributing to increased diffusion resistance [35]. A higher internal resistance necessitates a larger voltage response when assuming the same current, explaining why LIBs with reduced SOH show increased voltage response values. Such a resistance and voltage response to pulse test signals has been validated even in other battery chemistry [36], suggesting the effectiveness of using the pulse test to reveal the aging

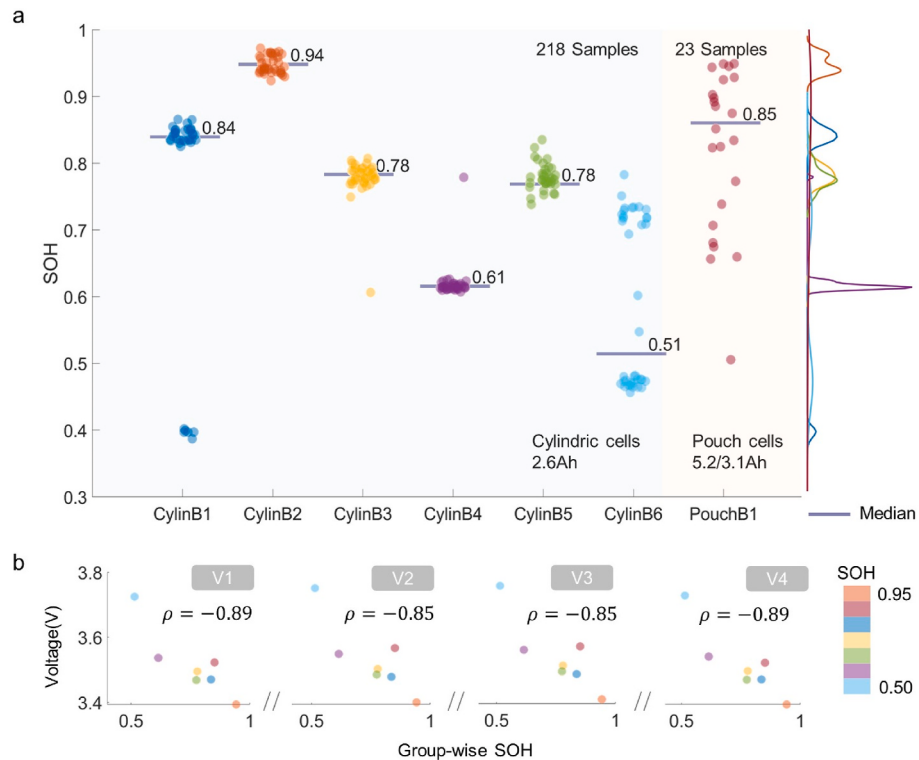


Fig. 4. Data visualization of the lab-testing cells. (a) SOH distribution in each group, with median SOH value, indicated. The jitters are added for the visibility of the points. (b) Scatter plot of the group-wise SOH median value and group-wise feature median value. The Pearson correlation is indicated. The features V_1 , V_2 , V_3 , and V_4 are selected for demonstration.

mechanism. The resistance rise increases polarization, the potential difference under non-equilibrium conditions, such as charging or discharging, especially at low SOC regions [37]. Polarization escalates with rising resistance and mass transport restrictions, leading to an increased voltage response value. Additional aging behaviors, such as lithium plating [38], indirectly affect voltage response, either by further increasing internal resistance or by reducing the available capacity, hence requiring higher voltage for the same power delivery. Despite the complex battery degradation mechanisms, we highlight that the extracted features are effective for diversified historical usage and physical patterns in a wide SOH range.

3.2. Prediction performance

3.2.1. The retired lab-testing cells

Having demonstrated the efficacy of the extracted features, the random forest model is trained to estimate the SOH of retired batteries from different groups. In Fig. 5(a), the parity plot shows a good diagnosis performance with sample points concentrated around the perfect line, corresponding to a 1.30% training error rate using the full feature model input. In Fig. 5(b), the testing error rate is 1.79%, slightly higher than the training result, attributed to one underestimated battery in the PouchB1 group. This can be rationalized by the fact that the median value of PouchB1 is up to 0.85, ranking the second place, while the SOH distribution within PouchB1 covers a considerably large SOH region, with the smallest value at 0.5 SOH level. We also examine the error distribution of the training set and testing set, respectively. In Fig. 5(c) and (d), the training and testing errors are nearly normally distributed, suggesting good predictability and stability in the model. Specifically, errors are symmetrically distributed around zero such that the model is equally likely to underestimate as it is to overestimate. However, the model tends to overestimate the CylinB6 due to a mismatch in the median SOH at 0.51 and SOH outlier values higher than 0.7. Such an

observation implies a practical difficulty in diagnosing the battery out of original data distributions. However, our model still shows a satisfying diagnosis regardless of the presence of heterogeneity in historical use and physical formats.

We have successfully estimated the SOH of retired batteries using extracted features from voltage response signals. It is intuitive to consider the feature contribution to successful diagnosis, which is of great interest to the model interpretability and model optimization. In contrast to analytically assessing the feature contribution when using full feature models, we select the features either independently or in their combinations and feed the selected features into the machine learning model to analyze the diagnosis performance.

In Table 2, the method column refers to selecting feature points from pulses. For instance, P1 refers to using the first four feature points, namely V_1 , V_2 , V_3 , and V_4 , as these points are extracted from the first applied pulse. The detailed feature extraction process can be found in Fig. 3(c). Similarly, P2 refers to using V_5 , V_6 , V_7 , and V_8 as model inputs. Note that for P5, one extra feature point is added, thus V_{17} , V_{18} , V_{19} , V_{20} and V_{21} are used as model inputs. The $P_i \sim P_j$ refers to concatenating the feature points from pulse P_i to pulse P_j . For example, eight feature points from V_1 to V_8 are used for P1~P2 method.

We observe the increased diagnosis performance on the training set when using a higher pulse magnitude. Specifically, the training error rate is 2.54%, 1.98%, 1.94%, 1.79%, and 1.41% when using the method from P1 to P5. According to Jiang et al. [37], they reported a higher polarization response on the voltage curve when using a higher constant current rate, especially under low SOC regions. Such observation adheres to Fig. 3(c) that the voltage response using 2A constant current is changing more significantly than using lower current values. As a result, the feature space when using a higher current rate will spread out, rather than concentrated in a specific value range, by amplifying the difference in the small internal resistance differences, facilitating machine learning models to learn potential battery degradation patterns. Additionally, we

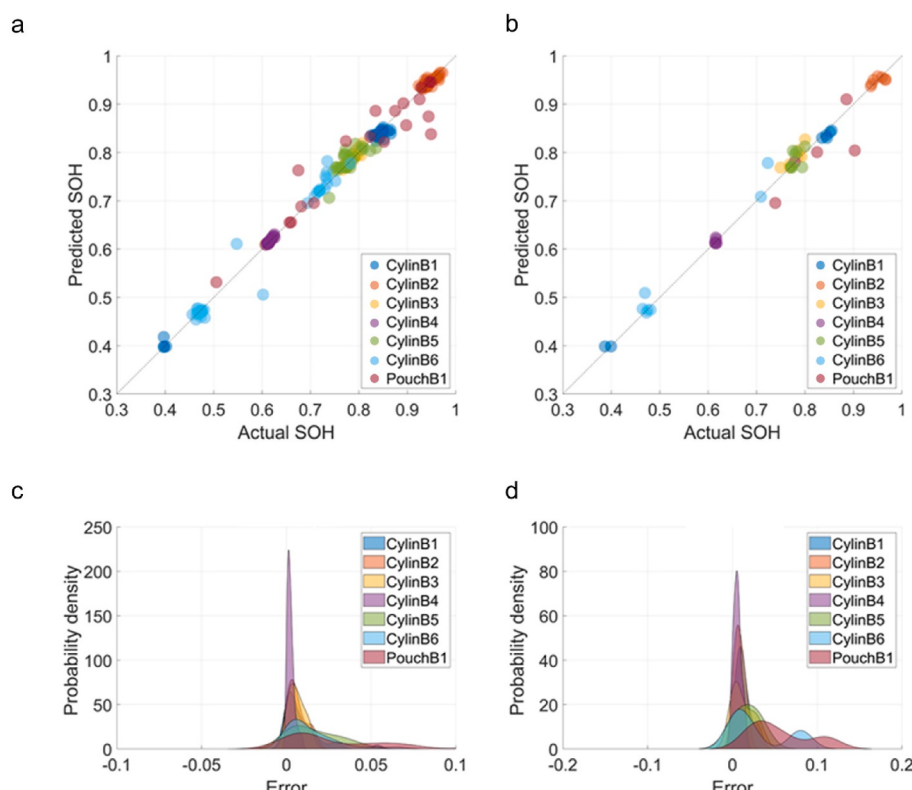


Fig. 5. Prediction results and error analysis using the full feature model using lab-testing cells. (a) Parity plot of the training set. (b) Parity plot of the testing set. (c) Probability density plot of error distribution on the training set. (d) Probability density plot of error distribution on the testing set.

Table 2

Prediction results with pulse selection and model hyperparameter optimization. The results are obtained by optimizing the model hyperparameters, namely the tree number K , the minimum leaf size θ , and the maximum split θ . The optimization time and pulse signal acquisition time are presented. The error rate follows a format of A(B)%, denoting the training and testing error, respectively.

Method	Err (%)	Time		Parameters K, θ, θ
		Optimization (ms)	Acquisition (s)	
P1	2.54 (2.97)	73.50	5	41,5,68
P2	1.98 (2.67)	19.70	5	4,2,46
P3	1.94 (3.47)	20.54	5	4,2,46
P4	1.79 (2.41)	19.87	5	4,2,46
P5	1.41 (3.30)	21.06	5	4,2,46
P1~P2	2.15 (2.77)	22.36	35	4,2,46
P1~P3	2.26 (3.12)	23.08	65	4,2,46
P1~P4	1.98 (2.49)	13.53	95	41,5,68
P1~P5	1.30 (1.79)	27.70	125	4,2,46
Regular	—	—	9000	—

also find discharging pulse results in a lower diagnosis error rate compared with the charging pulse at the same magnitude, which can be interpreted by the U-shape polarization-SOC relationship [37]. Specifically, using a charging pulse results in the polarization response tending to submerge toward a higher SOC region, where the polarization is less sensitive to the SOC variation when the same charging current is assumed. On the contrary, using a discharging pulse results in a more sensitive polarization response against the SOC variation, which enlarges the otherwise minor difference in internal resistance. Therefore, discharging pulses are more informative when the same current magnitude is assumed.

In addition to examining the effectiveness of a single pulse, we also evaluate the model performance by concatenating the different pulses. It is observed that the diagnosis error rate generally decreases by concatenating more pulses from P1 to P1~P5, despite a slight increase by using the P1~P3 method. Considering that the pulse signal is regarded as the Fourier series of sinusoidal signals in wide frequency regions, the pulse test reflects battery dynamics under wide timescales. Kowal et al. decoupled the distribution of relaxation time derived from voltage relaxation and observed the degradation trend in the charge transfer and diffusion process [24]. Given that the last two feature points in each pulse, for instance, V_3 , and V_4 in Pulse1, reflect the voltage relaxation, concatenating the pulses with different magnitudes brings in richer time scale degradation information, thus more accurate SOH diagnosis results.

Here we highlight the high efficiency of data acquisition time using our pulse test method to estimate the SOH of retired batteries. Even if we use the full feature model, i.e., the data acquisition time is 125s. Such a time is 98.6% shorter than the regular test, which requires 9000s to cover the entire 1C charging/discharging test and rest time. Moreover, the model optimization time is on the milliseconds level, thus it is applicable in practical applications for real-time usage. Furthermore, optimized hyperparameters show a high consistency, indicating the trained model is robust to the variations in model input, thanks to the effective feature engineering process. We also examine the effectiveness of the extracted feature by using other machine learning models with full features. Table 3 presents the diagnosis performance using linear regression, support vector machine (SVM), Gaussian process regression (GPR), and a neural network (NN) model, with the model hyperparameters recorded. The linear regression and SVM show comparable

Table 3

Diagnosis error rate using other machine learning models with full features, with the model hyperparameters recorded.

Model	Err rate (%)	Time (ms)	Hyperparameters
Linear	6.59 (7.99)	11.28	—
SVM	8.21 (7.48)	9.92	Linear kernel
GPR	1.09 (1.53)	368.65	Rational quadratic kernel, sigma = 0.02, beta = 0.75
NN	1.78 (2.10)	1111.98	1 layer fully connected, 10 neurons and tansig for hidden layer, purelin for output layer

time efficiency yet a higher diagnosis error rate, which is 6.59% (7.99%) and 8.21% (7.48%) for model training (testing), respectively. Although the GPR and NN methods show a comparable diagnosis error rate, the computation time is 13 and 40 times higher than that of the random forest model. As a result, the pulse test can effectively obtain the SOH of the retired batteries with comparable accuracy to regular capacity calibration tests while saving 98.6% time. The interpretable feature engineering not only shows good consistency in feature selection optimization but also in the examination of using other machine learning methods.

3.2.2. The retired electric vehicle cells

We have successfully demonstrated the effectiveness of the pulse method in diagnosing the SOH of retired lab-testing cells. However, despite the diversified historical usages, such cells have similar capacity designs and physical formats. Specifically, CylinB1 to CylinB6 groups are all in cylindric shape and with a nominal capacity of 2.6Ah. The retired electric vehicle cells can be much different in either capacity designs or physical formats, which challenges the retired battery SOH estimation by introducing more heterogeneities.

In Fig. 6, the prediction result and error analysis using retired electric vehicle cells (NCM cathode) and retired lab testing cells are demonstrated, where the pulse width is 5s. It is found that the as-trained model still performs well by producing a training and testing error lower than 1% and 10%, respectively. Even though such accuracy is slightly lower than that of the lab testing cells demonstrated in Fig. 5, the result is still acceptable noting that the capacity of such retired electric vehicle cells is 8 times larger than the lab testing ones. Moreover, the physical format is a pouch, which is different from that of the lab testing ones (cylindric). Given that capacity designs and physical formats drastically affect battery performance, we highlight the as-trained model, combined with pulse tests, is robust when battery parameter changes. The error distribution is also plotted for both lab testing and electric vehicle cells. It is noted that errors are normally distributed, indicating that the model has learned the shared pattern between the pouch and cylindric cells, despite very different capacity designs and historical usages.

As we highlight the SOH estimation at the recycling end as a highly heterogeneous data distribution problem, such heterogeneity also comes from the diversity in cathode material types. Here we used the LMO cells retired from electric vehicles with a nominal capacity of 10Ah as further validation. In Fig. 6, the prediction result and error analysis using retired electric vehicle cells (LMO cathode) and retired lab testing cells are demonstrated, where the pulse width is 5s. Despite the notable difference in operating voltage between NCM and LMO cells (e.g., such a difference is up to 0.5V), the model still produces a testing error rate of around 10%. Noting that the cathode material type, capacity design, and physical format are different from that of the lab testing cells, we conclude that the model successfully learned the commonalities of the voltage response from the pulse test. Also, the prediction error is normally distributed, indicating a well-trained model. In the actual recycling scenario, one integrated model will be adequate to process multiple types of retired batteries, thus saving the model training time

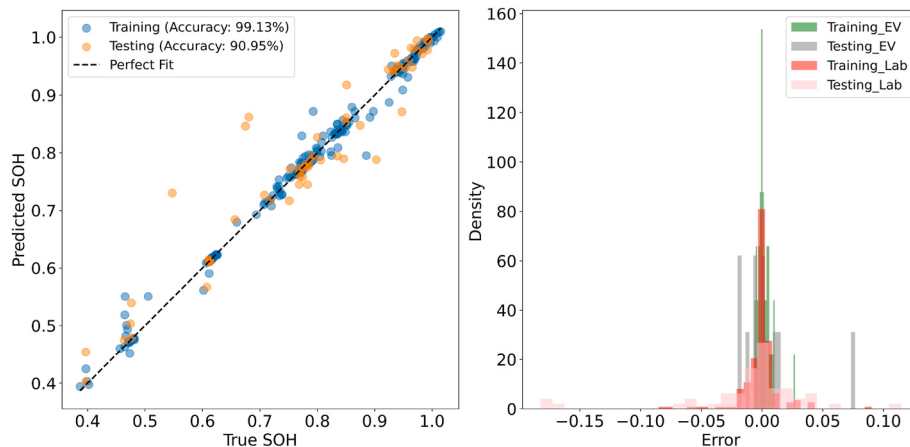


Fig. 6. Prediction results and error analysis (in Ah) using the full feature model for retired electric vehicle cells (NCM cathode) combined with retired lab testing cells. The pulse width is 5s.

and cost.

We further consider a more complex yet more realistic scenario, where lab testing cells and electric vehicle cells (NCM and LMO) are deliberately mixed up. In Fig. 8, the testing error is smaller than that demonstrated in Figs. 6 and 7, regardless of increasing complexities. We rationalize such a phenomenon that the as-trained model is less likely to be biased toward the lab testing cells whose sample size is otherwise larger than that of the electric vehicle cells. Therefore, future work should be done to collect more retired batteries in diversity rather than sample size.

In an actual battery recycling scenario, retired batteries not only come from multiple cathode material types but also come from multiple batches where data distribution and data sample size can be different. Herein, we use the Monte Carlo experiment to randomly shuffle the dataset to study the performance of the as-trained model under different batches. In Fig. 9, a sensitivity analysis is performed by varying the training set size (in percentage) and the shuffled data distribution. The scenario is the same as that has been demonstrated in Fig. 8, where lab testing cells and electric vehicle cells (NCM and LMO) are deliberately mixed up. In Fig. 9, the random seeds are from 0 to 99 using the numpy package. The solid lines are the median accuracy over these Monte Carlo runs and the standard deviations are plotted with shaded regions. It is expected that the prediction accuracy increases with the training data size since more data are utilized in the model training phase. Specifically, when the training size is 0.8 (i.e., 80% of the whole dataset), the median accuracy is 92.5%, with the best and the worst case being over

95% and 90%, respectively. Moreover, the model still produces an acceptable median prediction accuracy of around 82.5%, at a very low training data size of 0.2. The sensitivity analysis showcases the robustness of the pulse test, combined with the machine learning strategy, to random data distribution and changes in the access to data samples in the actual battery recycling scenario.

3.2.3. The effect of pulse width

Pulse width is an important parameter in pulse tests since it can influence the effectiveness of the pulse method. We have tested the retired electric vehicle batteries with a longer 10s pulse. Note that the batteries are unique ones rather than the same batteries being tested with different pulse widths. In Fig. 10, the lab testing cells and electric vehicle cells (NCM and LMO) are deliberately mixed up, which is identical to the setting in Fig. 8, other than that the pulse width is 10s. It is found that the model obtains comparable performance given testing error slightly decreases within 3%. We rationalize such an improvement by considering a larger voltage response difference brought by a longer charging time when the same SOH level is assumed. However, such an improvement is at the cost of 5s longer testing time per test, which should be jointly considered in the cost- and time-sensitive battery recycling industry practice.

3.2.4. The model performance in the unseen dataset

We also evaluate the model performance in unseen datasets. Considering factors such as cathode material types, physical formats,

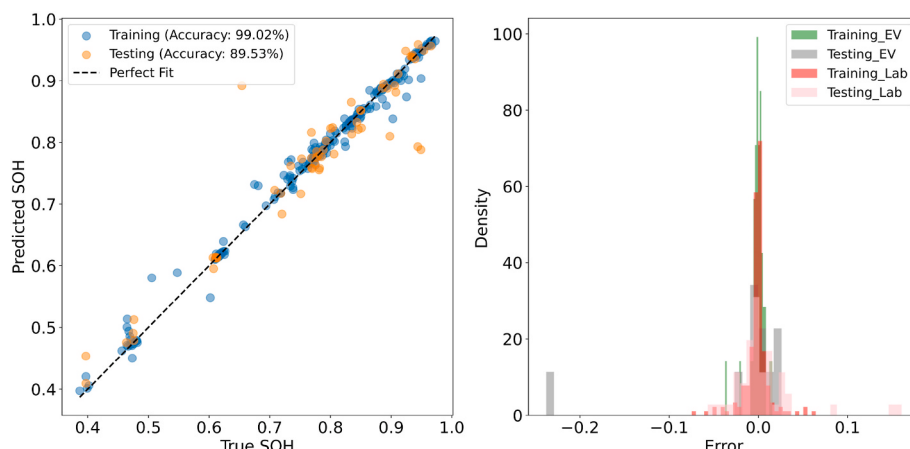


Fig. 7. Prediction results and error analysis (in Ah) using the full feature model for retired electric vehicle cells (LMO cathode) combined with retired lab testing cells. The pulse width is 5s.

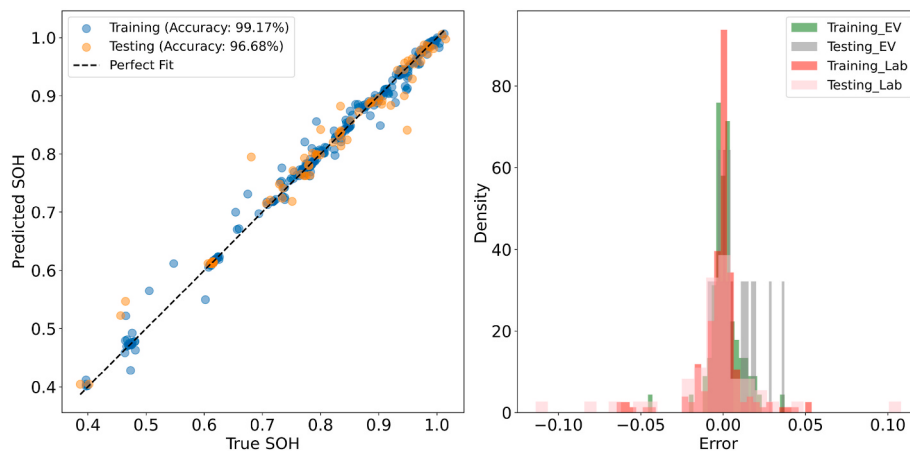


Fig. 8. Prediction results and error analysis (in Ah) using the full feature model for retired electric vehicle cells (NCM and LMO cathodes) combined with retired lab testing cells. The pulse width is 5s.

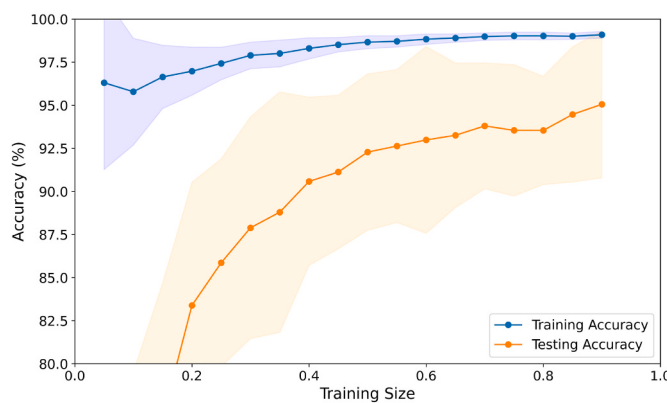


Fig. 9. Sensitivity analysis of prediction accuracy on the training data size (in percentage) from 5% to 95%, with 100 random Monte Carlo simulation runs. The random seeds are from 0 to 99 using the numpy package. The solid lines are the median accuracy over these runs and the standard deviations are plotted with shaded regions.

capacity designs, and historical operation conditions, we study the influences of historical operation conditions by exclusively splitting the dataset. Specifically, the CylinB1, CylinB4, CylinB5 and the CylinB2, CylinB3, CylinB6, are for training and testing, respectively.

In Fig. 11, the result shows that the model still produces an

acceptable prediction accuracy of up to 80% even if the testing data is completely unseen in the model training phase. Moreover, such an accuracy is very stable when data distribution is shuffled by Monte Carlo experiments. Interestingly, the model performance is generally better when the test data size is small (the training data size is large) in an asymptotic manner, suggesting that the battery recycler can minimize the cost of obtaining more samples while achieving satisfying prediction accuracy. Specifically, only using 20% of the training data (80% of the testing data) can achieve an accuracy of 80% on an unseen dataset. However, we note that the training and test datasets have identical cathode material types, capacity designs, and physical formats, and future work should be done to further generalize the as-trained model to even more complex scenarios.

3.3. Economic-environmental analysis

We have successfully demonstrated the effectiveness of the features extracted from the pulse test and the machine-learning method. Here we perform an economic-environmental analysis of the SOH pretreatment for hydrometallurgical, direct, and pyrometallurgical recycling methods using the pulse test. The retired battery type to be considered here is assumed to be the Panasonic 18650 PF NMC(622), with a nominal capacity of 2.88Ah and a weight of 46.5g. Considering average operation voltage being 3.9V, a 1A charging and discharging test for capacity calibration results in a 483kWh/t electricity consumption. We notice that such SOH pretreatment electricity is higher than the electricity

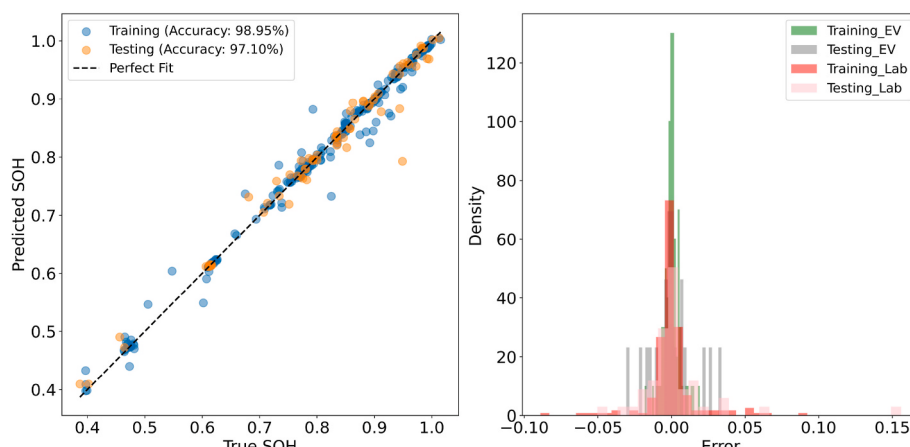


Fig. 10. Prediction results and error analysis (in Ah) using the full feature model for retired electric vehicle cells (NCM and LMO cathodes) combined with retired lab testing cells. The pulse widths are 5s for lab testing cells and 10s for retired electric vehicle cells, respectively.

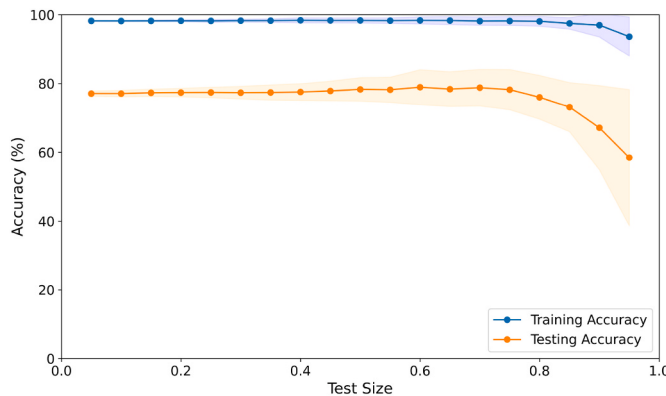


Fig. 11. The prediction accuracy on the unseen dataset, where the CylinB1, CylinB4, CylinB5 and the CylinB2, CylinB3, CylinB6, are for training and testing, respectively. Sensitivity analysis of prediction accuracy on the testing data size (in percentage) from 5% to 95%, with 100 random Monte Carlo simulation runs. The random seeds are from 0 to 99 using the numpy package. The solid lines are the median accuracy over these runs and the standard deviations are plotted with shaded regions.

consumption using the hydrometallurgical and direct recycling method, which are 500kWh/t and 300kWh/t, respectively [10]. For energy-intensive pyrometallurgical recycling, the electricity consumption is 1000kWh/t [10]. Since the battery recycler has no prior information on the collected batteries, a discharge step is necessary before a full-capacity calibration. As a result, the regular charging/discharging method needs even more electricity consumption and it is not feasible for practical battery recycling. In contrast, the pulse test significantly saves pretreatment time and electricity consumption. In Fig. 12(a), we analyze the pretreatment time ratio, i.e., the time needed for the pulse test and the regular charging/discharging. We assume the mean value of the initial SOC of the retired batteries to be 0.3. It is found that the pulse test saves at least 70% of the testing time compared with the 1A regular testing even if for the low SOH batteries. The time ratio using the pulse test and the regular test decreases asymptotically to 0.17 for high SOH

batteries since they are more time-consuming to calibrate. We also evaluate the electricity consumption for the pulse test and regular capacity calibration by calculating the electricity consumption ratio. When using the full feature model, i.e., all five pulses to perform SOH diagnosis, the electricity consumption is 0.58kWh/t, equivalently, 0.58kWh electricity for 21505 pieces of 18650 PF NMC(622) retired batteries. In Fig. 12(b), the electricity consumption ratio that compares the pulse test and regular capacity calibration is presented. The pulse test saves at least 82.7% of the electricity consumption even for low SOH batteries, which is 400kWh/t. We also find the electricity consumption ratio asymptotically decreases to 0.15 for the high SOH batteries. The asymptotic effect of the time ratio and electricity consumption ratio suggests that the pulse test gains advantages in high SOH regions. Considering that high SOH batteries have significant economic and environmental benefits for repurposing [4], the pulse test shifts otherwise time-consuming and cost-intensive SOH pretreatment into an affordable manner.

In Fig. 12(c), the carbon benefit of pulse test for the hydrometallurgical, direct, and pyrometallurgical recycling settings is presented. Carbon benefit refers to the carbon emissions of output materials minus the carbon emissions of input materials/electricity consumption. All recycling methods show a positive carbon benefit, suggesting that battery recycling is promising in reducing carbon emissions. However, the carbon benefit shows a decreasing trend for the pyrometallurgical recycling using the regular capacity calibration method, which indicates that the SOH sensitivity of equivalent carbon emission of products outweighs the input materials and chemical reagents. When using the pulse test for pretreatment, the carbon benefit of the pyrometallurgical recycling still shows a decreasing trend with SOH, even if it is higher than the carbon benefit when using the regular test. This suggests that pyrometallurgical recycling produces more carbon emissions for high SOH batteries [9]. For direct recycling, the amount of lithium supplementation dosage decreases with SOH, equivalently, the input material dosage decreases [10]. With product materials remaining unchanged, the carbon benefits, therefore, increase with SOH. For hydrometallurgical recycling, the excessive electricity consumption of the regular test leads to the downward trend of the carbon emission curve, which is otherwise with a rising trend with SOH when electricity carbon emission

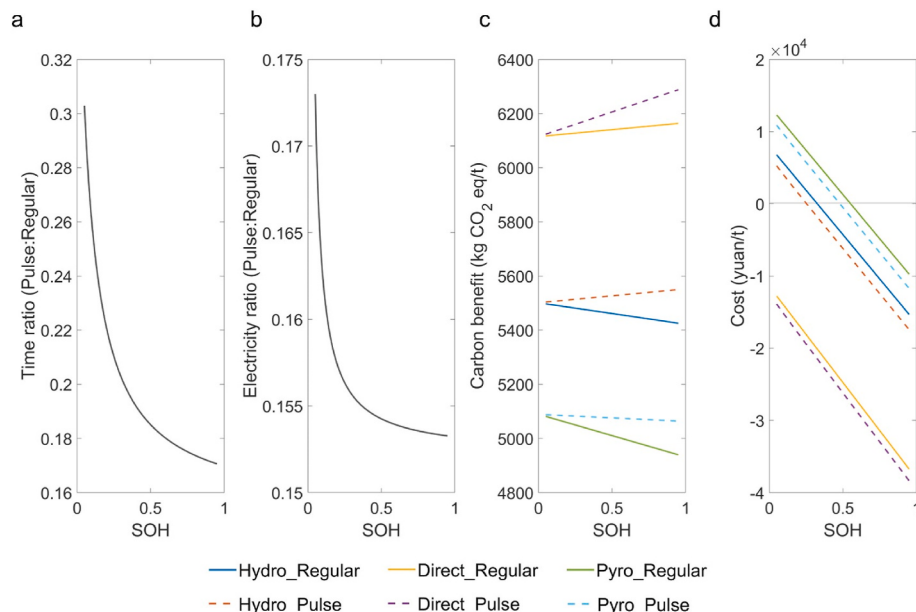


Fig. 12. Economic-environmental analysis. (a) Time ratio of pulse test time and regular charging/discharging time as a function of SOH. (b) Electricity ratio of pulse test time and regular charging/discharging time as a function of SOH. (c) Carbon benefits as a function of SOH for hydro, direct, and pyro recycling methods using pulse test and regular charging/discharging, respectively. (d) Cost as a function of SOH for hydro, direct, and pyro recycling methods using pulse test and regular charging/discharging, respectively. Negative cost stands for profit. Detailed calculation steps, recycling route, material price, and the material list can be found in the Supplementary Information.

is excluded. Thus, such a turnaround in the carbon benefit highlights the considerable carbon emission in the pretreatment, especially in high SOH regions using the regular test. When using the pulse test for SOH pretreatment, the carbon benefit for all the methods is offset up to a higher carbon benefit, highlighting that SOH pretreatment takes up a major electricity consumption contribution, consequently the carbon emission and electricity cost, to the overall recycling procedure. Assuming the average SOH of the retired batteries to be 0.5, the pulse test saves up to 65.43kg of CO₂ emission per ton of retired batteries. In Fig. 12(d), the cost as a function of SOH for hydrometallurgical, direct, and pyrometallurgical recycling methods using the pulse and regular test are presented, respectively, where negative costs refer to profits. It is observed that the hydrometallurgical and pyrometallurgical recycling methods require the SOH value of retired batteries to be higher than a certain threshold to make a profit, which contradicts the fact that retired batteries have low SOH. When using the pulse test for the SOH pretreatment, the cost curve generally shifts to a lower SOH region, thus reserving a larger SOH margin for recycling profit. With the increase of SOH, the cost decrease (equivalently, the profit increase) is amplified, which corresponds to the carbon benefit in Fig. 12(c) since the pulse test saves even more electricity consumption in high SOH regions. Assuming the average SOH of the retired batteries to be 0.5, the pulse test saves up to 1443.7 yuan (201.02 dollars) per ton of retired batteries. Notably, the cost is not as sensitive as the carbon benefit since the carbon benefit response of the regular and pulse test converges in a low SOH region. Such convergence can be rationalized by the fact that the impact of electricity price on recycling cost is smaller than that of carbon emissions resulting from electricity consumption. When electricity price rises, the impact of electricity on recycling costs under different SOH regions will increase, where a larger slope of the difference between the regular and pulse methods in Fig. 12(d) is anticipated. Similarly, when the carbon emission of the unit electricity consumption decreases, the difference in slope between the regular and pulse tests in Fig. 12(c) will shrink and approach a parallel manner. As the penetration of renewable energy sources increases in the future, all the recycling methods will be more sustainable and profitable due to the significant impact of electricity for pretreatment. The pulse test is promising in saving SOH pretreatment time and electricity consumption, thereby increasing the carbon benefit and the profitability of battery recycling.

4. Conclusion

This research presents a novel approach for diagnosing the SOH of retired LIBs, focusing especially on using field-available data at the cycling end rather than historical operational data. We collect 442 retired commercial LIBs from 4 manufacturers, 2 physical formats, 5 capacity designs, and 9 historical usages to build a diversified out-of-distribution retired battery dataset. We apply a fast pulse test to map the battery aging status. Simple yet effective features are extracted from the voltage response curve and used to instruct generalized random forest machine-learning models. The diagnosis error rates are 1.30% and 1.79% for training and testing, respectively. We have validated the effectiveness of the proposed method on retired electric vehicle batteries with different capacity designs and cathode materials (specifically, NCM and LMO). Moreover, the model can be generalized to unseen datasets, which are completely excluded during the training phase. A significant advantage is no prior information requirement on historical usage. Moreover, the pulse test saves at least 70% of the testing time compared with the regular capacity calibration test. We include an economic-technical analysis of carbon benefits and electricity consumption when using pulse tests for SOH pretreatment in pyrometallurgical, hydrometallurgical, and direct recycling settings. The findings suggest that the pulse test saves up to 1443.7 yuan (201.02 dollars) cost and 65.43kg of CO₂ emission per ton of retired batteries in pretreatment, assuming an average SOH of 0.5 of the retired batteries. This method shows great promise in reducing SOH pretreatment time and electricity

consumption, thus increasing carbon benefits, and boosting the profitability of battery recycling.

Though effective by injecting pulses at 5% SOC, future work should be done to investigate the validity of the pulse test under even lower SOC regions, saving more testing time. Also, the optimal pulse duration, magnitude, rest time, and suitableness for other cathode chemistries and diversified historical usages should be studied. The random retirement conditions, i.e., mixed cathode material types, SOC and SOH distributions should be considered to tackle the special challenges in battery recycling context. Mechanism-informed SOH diagnosis is recommended for recycling pretreatment by investigating the microscopic degradation such as crystal structures, impurity phases, structural mismatches, and morphological patterns with data-driven and machine-learning methods. Nevertheless, by providing a faster, more accurate method for diagnosing the SOH of retired batteries, this research contributes to efficient and profitable battery recycling. It paves the way for better recycling of retired LIBs, thereby reducing waste and enhancing the sustainability of the entire battery lifecycle. This work underscores the importance of using pulse tests and machine learning in battery health diagnosis, especially for highly heterogeneous battery recycling pretreatment.

CRediT authorship contribution statement

Shengyu Tao: Conceptualization, Data curation, Methodology, Software, Writing – original draft, Writing – review & editing. **Ruifei Ma:** Methodology, Validation. **Yiou Chen:** Data curation, Investigation. **Zheng Liang:** Methodology. **Haocheng Ji:** Data curation, Investigation, Methodology. **Zhiyuan Han:** Methodology. **Guodan Wei:** Investigation, Supervision. **Xuan Zhang:** Conceptualization, Data curation, Formal analysis, Funding acquisition, Investigation, Methodology, Writing – original draft, Writing – review & editing. **Guangmin Zhou:** Conceptualization, Data curation, Formal analysis, Funding acquisition, Investigation, Methodology, Project administration, Supervision, Writing – original draft, Writing – review & editing.

Declaration of competing interest

The authors declare that they have no known competing financial interests or personal relationships that could have appeared to influence the work reported in this paper.

Data availability

Data will be made available on reasonable request from corresponding authors.

Acknowledgments

This work was supported by Shenzhen Science and Technology Program (Grant No. KQTD20170810150821146), Key Scientific Research Support Project of Shanxi Energy Internet Research Institute (Grant No. SXEI2023A002), Tsinghua Shenzhen International Graduate School Interdisciplinary Innovative Fund (Grant No. JC2021006), Shenzhen Ubiquitous Data Enabling Key Lab (Grant No. ZDSYS20220527171406015), Joint Funds of the National Natural Science Foundation of China (Grant No. U21A20174), Guangdong Innovative and Entrepreneurial Research Team Program (Grant No. 2021ZT09L197), and National Key Research and Development Program of China (Grant No. 2021YFB2500200).

Appendix A. Supplementary data

Supplementary data to this article can be found online at <https://doi.org/10.1016/j.jpowersour.2024.234156>.

References

- [1] C.-Y. Wang, T. Liu, X.-G. Yang, S. Ge, N.V. Stanley, E.S. Rountree, et al., Fast charging of energy-dense lithium-ion batteries, *Nature* 611 (2022) 485–490.
- [2] J. Schmalstieg, S. Käbitz, M. Ecker, D.U. Sauer, A holistic aging model for Li (NiMnCo)O₂ based 18650 lithium-ion batteries, *J. Power Sources* 257 (2014) 325–334.
- [3] M. Cheng, A. Ran, X. Zheng, X. Zhang, G. Wei, G. Zhou, et al., Sustainability evaluation of second-life battery applications in grid-connected PV-battery systems, *J. Power Sources* 550 (2022) 232132.
- [4] M. Cheng, X. Zhang, A. Ran, G. Wei, H. Sun, Optimal dispatch approach for second-life batteries considering degradation with online SoH estimation, *Renew. Sustain. Energy Rev.* 173 (2023) 113053.
- [5] J. Ma, J. Wang, K. Jia, Z. Liang, G. Ji, Z. Zhuang, et al., Adaptable eutectic salt for the direct recycling of highly degraded layer cathodes, *J. Am. Chem. Soc.* 144 (2022) 20306–20314.
- [6] Y. Yao, M. Zhu, Z. Zhao, B. Tong, Y. Fan, Z. Hua, Hydrometallurgical processes for recycling spent lithium-ion batteries: a critical review, *ACS Sustain. Chem. Eng.* 6 (2018) 13611–13627.
- [7] B. Makuzo, Q. Tian, X. Guo, K. Chattopadhyay, D. Yu, Pyrometallurgical options for recycling spent lithium-ion batteries: a comprehensive review, *J. Power Sources* 491 (2021) 229622.
- [8] J. Wang, K. Jia, J. Ma, Z. Liang, Z. Zhuang, Y. Zhao, et al., Sustainable upcycling of spent LiCoO₂ to an ultra-stable battery cathode at high voltage, *Nat. Sustain.* 6 (2023) 797–805.
- [9] M. Zheng, H. Salim, T. Liu, R.A. Stewart, J. Lu, S. Zhang, Intelligence-assisted predesign for the sustainable recycling of lithium-ion batteries and beyond, *Energy Environ. Sci.* 14 (2021) 5801–5815.
- [10] G. Ji, J. Wang, Z. Liang, K. Jia, J. Ma, Z. Zhuang, et al., Direct regeneration of degraded lithium-ion battery cathodes with a multifunctional organic lithium salt, *Nat. Commun.* 14 (2023) 584.
- [11] S. Tao, H. Liu, C. Sun, H. Ji, G. Ji, Z. Han, et al., Collaborative and privacy-preserving retired battery sorting for profitable direct recycling via federated machine learning, *Nat. Commun.* 14 (2023) 8032.
- [12] K.S. Ng, C.-S. Moo, Y.-P. Chen, Y.-C. Hsieh, Enhanced coulomb counting method for estimating state-of-charge and state-of-health of lithium-ion batteries, *Appl. Energy* 86 (2009) 1506–1511.
- [13] K.K. Sadabadi, X. Jin, G. Rizzoni, Prediction of remaining useful life for a composite electrode lithium ion battery cell using an electrochemical model to estimate the state of health, *J. Power Sources* 481 (2021) 228861.
- [14] M.-K. Tran, M. Mathew, S. Janhunen, S. Panchal, K. Raahemifar, R. Fraser, et al., A comprehensive equivalent circuit model for lithium-ion batteries, incorporating the effects of state of health, state of charge, and temperature on model parameters, *J. Energy Storage* 43 (2021) 103252.
- [15] Y. Zhang, Q. Tang, Y. Zhang, J. Wang, U. Stimming, A.A. Lee, Identifying degradation patterns of lithium ion batteries from impedance spectroscopy using machine learning, *Nat. Commun.* 11 (2020) 1706.
- [16] Z. Deng, X. Hu, P. Li, X. Lin, X. Bian, Data-driven battery state of health estimation based on random partial charging data, *IEEE Trans. Power Electron.* 37 (2021) 5021–5031.
- [17] A. Weng, E. Dufek, A. Stefanopoulou, Battery passports for promoting electric vehicle resale and repurposing, *Joule* 7 (2023) 837–842.
- [18] Y. Jiang, J. Jiang, C. Zhang, W. Zhang, Y. Gao, N. Li, State of health estimation of second-life LiFePO₄ batteries for energy storage applications, *J. Clean. Prod.* 205 (2018) 754–762.
- [19] X. Xiao, L. Wang, Y. Wu, Y.-Z. Song, Z. Chen, X. He, Cathode Regeneration and Upcycling of Spent LIBs: toward Sustainability, *Energy & Environmental Science*, 2023.
- [20] X. Lai, C. Deng, J. Li, Z. Zhu, X. Han, Y. Zheng, Rapid sorting and regrouping of retired lithium-ion battery modules for echelon utilization based on partial charging curves, *IEEE Trans. Veh. Technol.* 70 (2021) 1246–1254.
- [21] E. Braco, I. San Martín, P. Sanchis, A. Ursúa, D.-I. Stroe, State of health estimation of second-life lithium-ion batteries under real profile operation, *Appl. Energy* 326 (2022) 119992.
- [22] E. Braco, I. San Martin, P. Sanchis, A. Ursúa, D.-I. Stroe, Health indicator selection for state of health estimation of second-life lithium-ion batteries under extended ageing, *J. Energy Storage* 55 (2022) 105366.
- [23] M. Faraji-Niri, M. Rashid, J. Sansom, M. Sheikh, D. Widanage, J. Marco, Accelerated state of health estimation of second life lithium-ion batteries via electrochemical impedance spectroscopy tests and machine learning techniques, *J. Energy Storage* 58 (2023) 106295.
- [24] E. Goldammer, J. Kowal, Determination of the Distribution of Relaxation Times by Means of Pulse Evaluation for Offline and Online Diagnosis of Lithium-Ion Batteries, 2021. Batteries.
- [25] F. Luo, H. Huang, L. Ni, T. Li, Rapid prediction of the state of health of retired power batteries based on electrochemical impedance spectroscopy, *J. Energy Storage* 41 (2021) 102866.
- [26] H. Quinard, E. Redondo-Iglesias, S. Pelissier, P. Venet, Fast electrical characterizations of high-energy second life lithium-ion batteries for embedded and stationary applications, *Batteries* 5 (2019) 33.
- [27] K. He, S. Tao, S. Fu, H. Fan, Y. Tao, Y. Wang, et al., A novel quick screening method for the second usage of parallel-connected lithium-ion cells based on the current distribution, *J. Electrochem. Soc.* 170 (2023) 030514.
- [28] Li T, Zhou Z, Thelen A, Howey D, Hu C. Predicting Battery Lifetime under Varying Usage Conditions from Early Aging Data. arXiv preprint arXiv:230708382. 2023.
- [29] S. Tao, C. Sun, S. Fu, Y. Wang, R. Ma, Z. Han, et al., Battery cross-operation-condition lifetime prediction via interpretable feature engineering assisted adaptive machine learning, *ACS Energy Lett.* (2023) 3269–3279.
- [30] S. Fu, S. Tao, H. Fan, K. He, X. Liu, Y. Tao, et al., Data-driven capacity estimation for lithium-ion batteries with feature matching based transfer learning method, *Appl. Energy* 353 (2024) 121991.
- [31] A. Ran, Z. Liang, S. Chen, M. Cheng, C. Sun, F. Ma, et al., Fast clustering of retired lithium-ion batteries for secondary life with a two-step learning method, *ACS Energy Lett.* 7 (2022) 3817–3825.
- [32] A. Ran, M. Cheng, S. Chen, Z. Liang, Z. Zhou, G. Zhou, et al., Fast remaining capacity estimation for lithium-ion batteries based on short-time pulse test and Gaussian process regression, *ENERGY & ENVIRONMENTAL MATERIALS* 6 (2023) e12386.
- [33] D.I. Stroe, M. Swierczynski, S.K. Kær, R. Teodorescu, Degradation behavior of lithium-ion batteries during calendar ageing—the case of the internal resistance increase, *IEEE Trans. Ind. Appl.* 54 (2018) 517–525.
- [34] M.R. Segal, Machine Learning Benchmarks and Random Forest Regression, 2004.
- [35] L. Liu, J. Park, X. Lin, A.M. Sastry, W. Lu, A thermal-electrochemical model that gives spatial-dependent growth of solid electrolyte interphase in a Li-ion battery, *J. Power Sources* 268 (2014) 482–490.
- [36] S. Tao, H. Fan, Y. Lei, X. Xu, Y. Sun, B. You, et al., The proactive maintenance for the irreversible sulfation in lead-based energy storage systems with a novel resonance method, *J. Energy Storage* 42 (2021) 103093.
- [37] J. Jiang, Q. Liu, C. Zhang, W. Zhang, Evaluation of acceptable charging current of power Li-ion batteries based on polarization characteristics, *IEEE Trans. Ind. Electron.* 61 (2014) 6844–6851.
- [38] Z.M. Konz, E.J. McShane, B.D. McCloskey, Detecting the onset of lithium plating and monitoring fast charging performance with voltage relaxation, *ACS Energy Lett.* 5 (2020) 1750–1757.
- [39] S. Tao, H. Liu, C. Sun, et al., Collaborative and privacy-preserving retired battery sorting for profitable direct recycling via federated machine learning, *Nat. Commun.* 14 (2023) 8032. <https://doi.org/10.1038/s41467-023-43883-y>.